Nonlinear Interaction of Bernstein Mode*)

in Beam-Plasma System

Toshitaka IDEHARA**

(Received Oct. 15, 1969)

When the Bernstein mode is excited strongly in the magnetoplasma penetrated by the gyrating electron beam, it is observed that the harmonics of this mode are produced due to the nonlinear interaction. Observations have been made of: the spatial behabior of the fundamental and harmonic waves along the axitial and radial directions for various intensities of the beam, the diffusion of the plasma across the magnetic field and the frequency power spectrum at the fundamental and its harmonics. It is verified from these observations, that for the fairly intense electron beam, the Bernstein mode grows exponentially along the magnetic field (linear state), reaches its saturation level with together the generation of the harmonics confined in the beam plasma region (nonlinear state) and then, these waves decay and are broadened, the system removing to the turbulence-like state with the diffusion of ion.

1 Introduction

A theoretical investigation of the instability, which results in an excitation of the Bernstein mode, has been carried out in details by several authors[1)-3)]. This instability, which is an absolute one, results from the anisotropy of the electron distribution in velocity space and one of the possibilities of this instability is the case of the Maxwellian plasma penetrated by the gyrating electron beam.

The experimental study of this instability has been done by using the low pressure dc discharge where the electron beam is considered to exist spontaneously[4)5)] or by using the plasma generated by the ionization of the neutral gas due to the injection of the electron beam,[6)7)] and the excitation of electron harmonics which result from the instability have been observed up to several tenth. As described in our previous paper[8)], we also investigated this phenomenon by injecting the gyrating electron beam into the plasma in nearly thermal equilibrium. As the parameters of the beam and plasma are varied independently, we have obtained the more detailed imformations about this instability. It will be described in this paper, that when we inject the more intense electron beam, the harmonics of the Bernstein mode are generated as the result of the nonlinear interaction of this mode, and these waves (fundamental and harmonic) grow spatially, reaches

*) Reported in part in J. Phys. Soc. Japan **25** (1968) 927.

** Dep. of Applied Physics

their saturation levels at certain points and decay with spread of each peak in the spectrum and then, the turbulence-like state is attained.

Recently, Apel[9] reported in detail that when the instability ascribed to the coupling of the slow space charge wave with the plasma wave or the cyclotron wave developed, the harmonics of them were generated and the system becomes turbulence-like.

In §2, is described the experimental apparatus and procedure together with the properties of the plasma and the beam. In §3, the experimental results are shown and in §4, the discussions about the results is described.

2 Experimental apparatus and procedure

In order to obtain the beam-plasma system where the Maxwellian plasma is penetrated by a gyrating electron beam, we set up the apparatus as shown in Fig. 1, which is similar to that shown in Ref. 8 but is improved fairly. It is consisted of three regions, that is, the dc discharge region, the plasma diffused region and the beam-produced region. Argon gas of the pressure of $P_1 \approx 10^{-1}$ *Torr* is fed into the discharge region and, by using a method of differential pumping, the gas pressure of the plasma diffused and the beam-produced regions are maintained at $P_2 \approx 7 \times 10^{-4}$ and $P_3 \approx 5 \times 10^{-6}$ *Torr*, respectively. An external magnetic field is applied along the tube axis by the coil I and coil II and an example of its intensity distribution on the axis is shown in Fig. 1. The field produced by the coil I in the plasma diffused region is uniform (1 percent) within 30 *cm* from the inlet of a beam and is varied from 290 to 3800 *gauss*. In the discharge region the plasma is produced by a dc discharge between cathode and anode situated beyond the coil II and diffused through a hole (12 *mm* in diameter and 200 *mm* in length) at the center of the coil

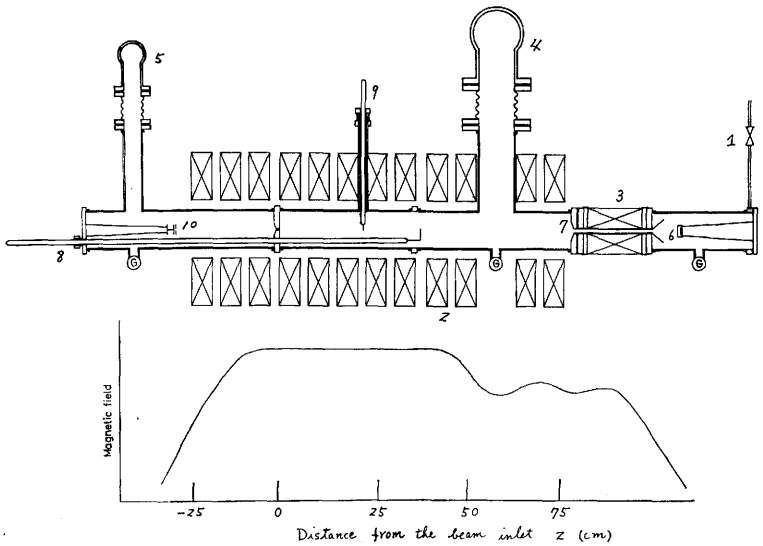

Fig. 1. Experimentel set up and the intensity of the magnetic field along the axis: 1) gas inlet ; 2) coil I ; 3) coil II ; 4) 4″ diffusion pump ; 5) 2″ diffusion pump ; 6) cathode; 7) anode; 8) coaxitial probe I; 9) coaxitial probe II; 10) electron gun.

and anode into the plasma diffused region along the field produced by the coil II. The diffused plasma is maintained along the axis of the glass tube (100 *mm* in diameter) by the external magnetic field. The discharge current I_d can be varied from 20 *mA* to 4 *A*, so that the plasma density varies from $5 \times 10^{10} cm^{-3}$ to $1 \times 10^{12} cm^{-3}$. In Fig. 2(a), are shown the space potential V_s (where the anode is grounded), the electron temperature T_e observed by the Langmuir probe and the ion saturation current I_i where the probe potential is set at -75 V as functions of the distance z from the beam inlet, where the electron beam is not injected. V_s and T_e are constant within experimental error, while I_i decreases by about 30 percent near the beam inlet.

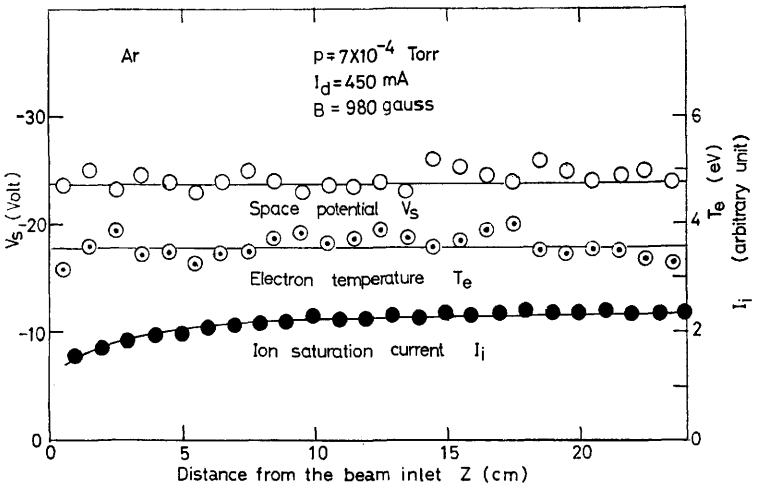

Fig. 2.(a) The space potential V_s, the electron temperature T_e and the ion saturation current I_i as functions of z.
Ar, $p_2 = 7 \times 10^{-4}$ *Torr*. $I_d = 450$ *mA*. $B = 980$ *gauss*.

On the other hand, in Fig. 2(b) are shown V_s and T_e as functions of the radial distance r from the axis at $z = 17cm$, where the beam is not injected. When the electron beam ($V_b = 610$ *V*, $I_b = 16$ *mA*) is injected into, the curve of V_s is replaced by the dotted one, while T_e remains unchanged. The variation of I_i along the radial direction is described in detail in the following paragraph (Refer to Fig. 13), when the intensity of the beam is varied.

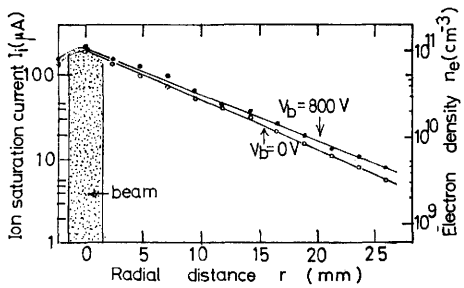

Fig. 2.(b) The ion saturation current I_i as functions of r at $z = 17cm$.

An electron beam is produced by the Pierce gun in the beam produced region and is injected into the plasma diffused region through a hole which is 3 *mm* in diameter and 10 *mm* in length. As described in Ref. 8, the gun is set outside the coil I so that the electron ejected from the gun feels the increasing magnetic field as it runs to the plasma diffused region and, therefore, a part of the initial energy of the electron is transformed to the energy perpendicular to the magnetic field.

When the voltage of the beam V_b is changed from 100 V to 1200 V, the current of the beam I_b changes from 3 mA to 46 mA. (The perveance of the gun being about 2×10^{-6} $AV^{-3/2}$) and then, the density n_b of the beam changes from about $1.2\times10^{8}cm^{-3}$ to $5.3\times10^{8}cm^{-3}$.

Microwave emission from the beam-plasma system are picked up by two coaxial probe (one of them is movable along the axial direction (probe I) and the other along the radial direction (probe II)) and received by radiometers which are operated at the several receiving frequencies f and have the band width of 5 MHz. The output power of the radiometer is plotted as a function of the magnetic field on the XY-recorder continuously with I_d, V_b (I_b), axitial situation z and radial situation r as parameters. When the accurate power of the emission intensity is measured, its power is calibrated by that of noise standard, P_{ns}, which is blackbody emission from an Ar discharge plasma in a thermal equilibrium with $T_e=1.14\times10^{4}$ $^{\circ}K$.

3 Experimental results

3.1 Observation of the harmonics of the Bernstein mode

It has been described in Ref. 8, that the Bernstein mode (denoted by CHW there) is excited strongly, when the gyrating electron beam is injected into the plasma in nearly thermal equilibrium in which the wave is not excited and the emission power is comparable with that of the thermal noise.

When the beam is more intense, it is observed that the harmonics of this mode are generated by the nonlinear coupling. In Fig. 3, are shown emission spectra as functions of the magnetic field for four different receiving frequencies. In the curve (a) for $f_1=4$ GHz, the strongly enhanced emissions refered to the excitation of the Bernstein mode are seen near $f_c/f_1=1/2$ and 1/3. The curves (b), (c) and (d) show the emission spectra for the receiving frequencies $f_2=8$ GHz ($=2f_1$), $f_3=12$ GHz ($=3f_1$) and $f_6=24$ GHz ($6f_1$), respectively. In these four curves, the emission peaks denoted by A, B, C and D are observed at the same magnetic field of $f_c/f_1\approx1/2$, while their powers become weak as the receiving frequency increases, that is, the powers of peaks A, B, C and D are larger than that from the noise standard by 50 dB, 36 dB, 21 dB and 8 dB, respectively. Since the plasma is so tenuous for three frequencies of f_2, f_3 and f_6, that the Bernstein mode cannot be observed usually, peaks B, C and D may be ascribed to the second, the third and the sixth harmonics of the peak A.

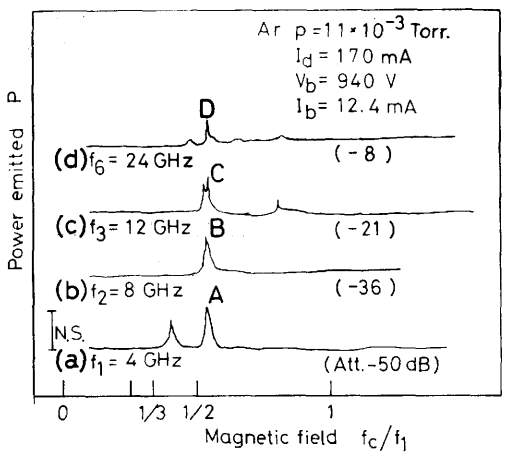

Fig. 3. Emission spectra for four receiving frequencies as functions of the magnetic field. Ar, $p_2=1\times10^{-3}$ $Torr$. $I_d=170$ mA. $V_b=940$ V. $I_b=12.4$ mA.

In Fig. 4 (a) and (b), the magnetic field,

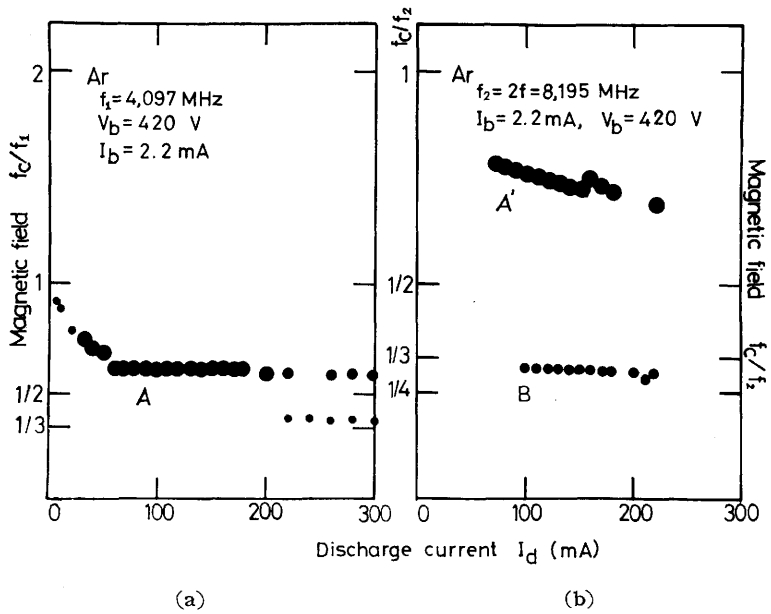

Fig. 4. The magnetic field f_c/f, where the emission is observed, is plotted as functions of the discharge current I_d, (a) for the case of $f=f_1$ and (b) for the case of $f=f_2$, respectively. $V_b=420$ V. $I_b=2.2$ mA.

where the enhanced emission peaks A and B are observed, are plotted as a function of the discharge current I_d. Note that the points denoted by A' in Fig. 4 (b), which appear in the range of $1/2<f_c/f_2<1$, correspond to the emission peaks refered to the Bernstein mode for the frequency f_2. In Fig. 4 (c), the emission powers of peaks A, B and C compared with that from the noise standard are plotted as functions of the discharge current I_d. It is clear from these figures that the discharge current I_d is varied, the peaks A and B always appear at the same magnetic field and the variations of their peak powers are quite similar while the former is larger by about 30 dB than the latter.

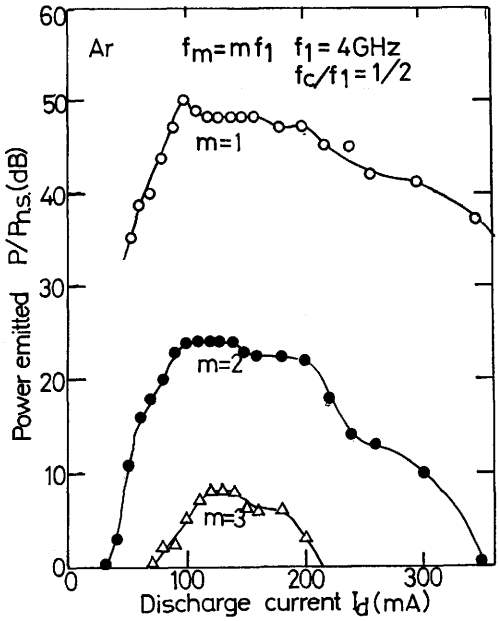

Fig. 4.(c) The emission power P/P_{ns} near $f_c/f=1/2$, is plotted as functions of the discharge current I_d, for the cases of f_1, f_2 and f_3. $V_b=420$ V. $I_b=2.2$ mA.

Further, from the simultaneous observation of two emissions corresponding to peaks A and B on a dual beam shynchroscope, it is confirmed that both are emitted not stationarily but as pulses whose widths are several microsecond, and the pulses

corresponding to both peaks always occur at the same time.

These experimental results prove that the peaks B, C and D are generated as harmonics of the peak A.

3.2 Measurement of the spatial behavior

In Fig. 5, the emission powers of peaks A, B and C are shown as a function of the distance r along the radial direction from the axis at z=17 *cm*, together with the plasma density n_p obtained by the measurement of the ion saturation current I_i. (We will discuss in §3.4 in detail about the difference between the slopes of n_p in the both cases with (V_b =800 *V*) and without (V_b=0 *V*) the electron beam.) It must be noted in this figure, that the fundamental wave (peak A) is excited in the beam-plasma region and can propagate to the plasma region across the boundary between both region, while the harmonic waves (peaks B and C) are generated in the former region and are confined there.

In Fig. 6, the variation of the emission powers of the peaks (A, B and C) along the axis are shown as functions of the axial distance z from the beam inlet. It is seen in this figure that the fundamental wave (peak A) starts to be excited at a certain distance z_{st}, grows exponentially, reaches their saturation level at the distance z_{sa} and then tends to decay, while for the harmonic waves (peak Band C), the higher the frequency, the further along the axis do they show the same behavior as the fundamental.

In Fig. 7, the distance z_{st} and z_{sa}, where the waves start to grow and reach their saturation levels, are plotted as functions of the beam voltage V_b for the waves corresponding

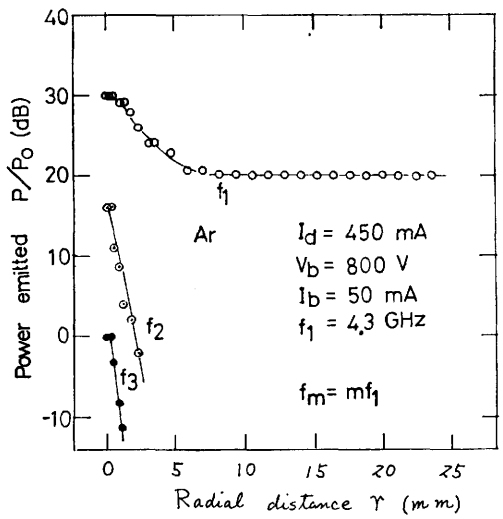

Fig. 5. The emission power P/P_{ns} is plotted as functions of radial distance from the axis r for the cases of f_1, f_2 and f_3, together with the distribution of the plasma density along the radial direction. I_d=450 *mA*. V_b=800 *V*. I_b=50 *mA*.

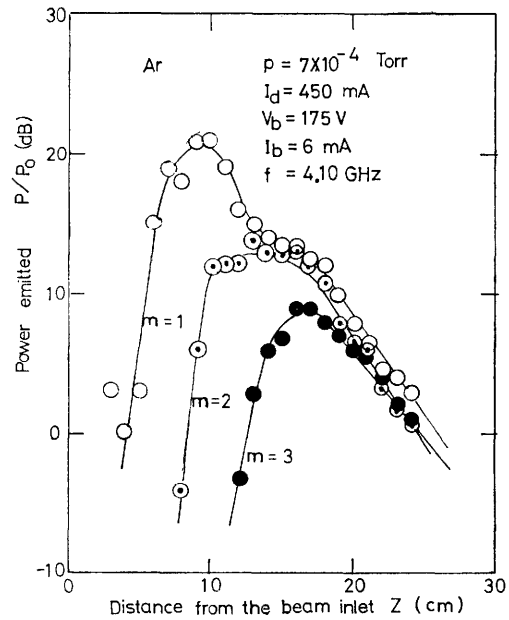

Fig. 6. The emission power P/P_{ns} is plotted as functions of the axitial distance from the beam inlet z for the cases of f_1, f_2 and f_3. I_d=450 *mA*. V_b= 175 *V*. I_b=6 *mA*.

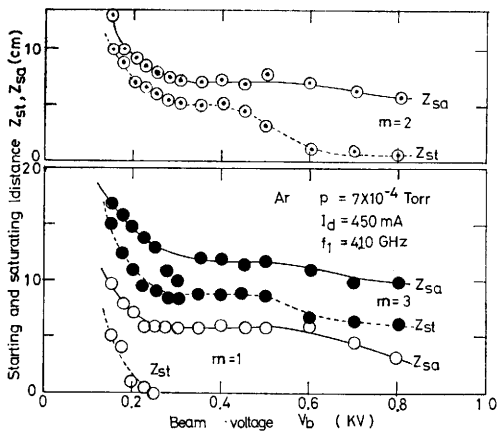

Fig. 7. Starting and saturating distances, z_{st} and z_{sa} are plotted as functions of V_b for the cases of f_1, f_2 and f_3. Ar, $p_2 = 7 \times 10^{-4}$ *Torr*. $I_d = 450$ *mA*.

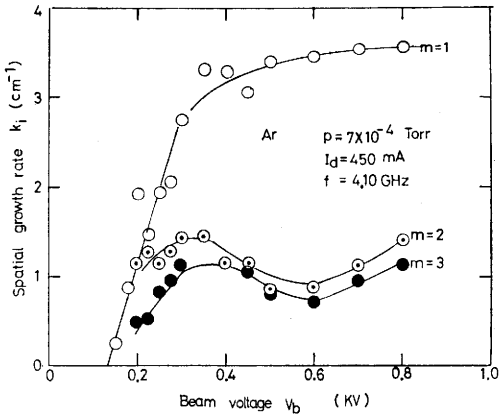

Fig. 8. Spatial growth rate k_i is plotted as functions of V_b for the cases of f_1, f_2 and f_3. Ar, $p_2 = 7 \times 10^{-4}$ *Torr*. $I_d = 450$ *mA*.

to the peaks A, B, and C. (Here, the beam current I_b varies as $V_b^{3/2}$ and the beam density varies as V_b.) It is seen in this figure that both z_{st} and z_{sa} for the three waves become shorter, with increasing V_b.

In Fig. 8, the spatial growth rate k_i in the range between z_{st} and z_{sa} for three waves are shown as functions of V_b. It is known that k_is become large with increasing V_b and tend to saturate at $V_b \approx 400$ *V*. In Fig. 9, the normalized half value widths in magnetic field $\Delta B/B$ for the peaks A, B, and C are shown as functions of z. It shows that $\Delta B/B$ is increased rapidly beyond the saturation distance z_{sa}, which is shown by arrows in this figure (where the value of z_{sa} shown in Fig. 7 are used.)

3.3 *Variation of the emission power with the intensity of the beam*

The emission powers of the peaks A, B, C and D are measured for the various values of the beam voltage V_b. As shown in Fig. 10, when V_b increases, the power P for f_1 (peak A) is increased and then saturated, and also, peak powers at harmonics (f_2, f_3 and f_6) are saturated at the larger V_b.

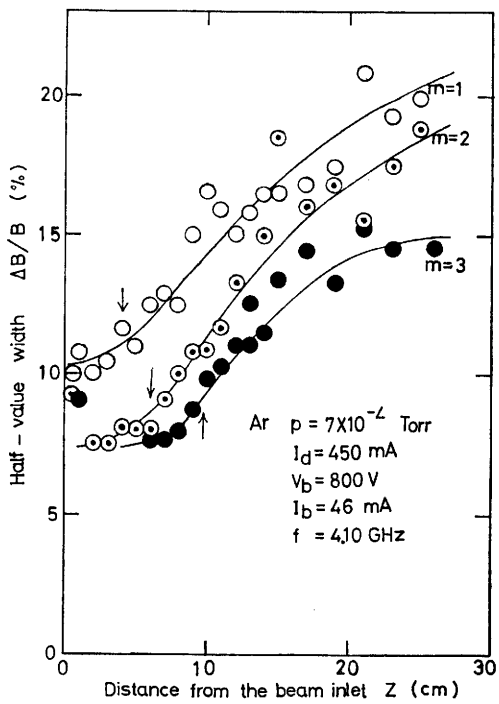

Fig. 9. Half value width $\Delta B/B$ is plotted as functions of z for the peaks A, B and C. Ar, $p_2 = 7 \times 10^{-4}$ *Torr*. $I_d = 450$ *mA*. $V_b = 800$ *V*. $I_b = 46$ *mA*.

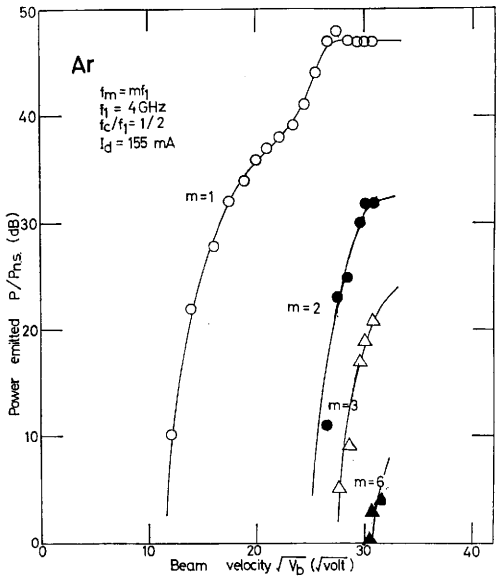

Fig. 10. The emission power P/P_{ns} is plotted as functions of $\sqrt{V_b}$ for the cases of f_1, f_2, f_3 and f_6. $I_d = 155$ mA.

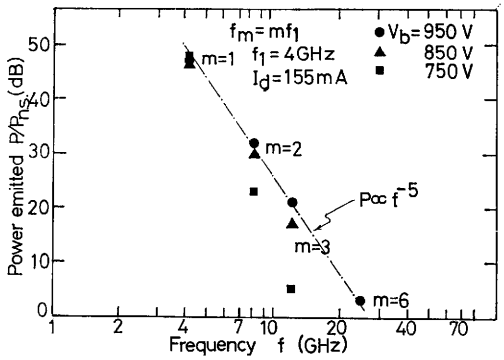

Fig. 11. The emission power P/P_{ns} of peaks A, B, C and D as functions of the frequency f, with V_b as parameter. $I_d = 155$ mA,

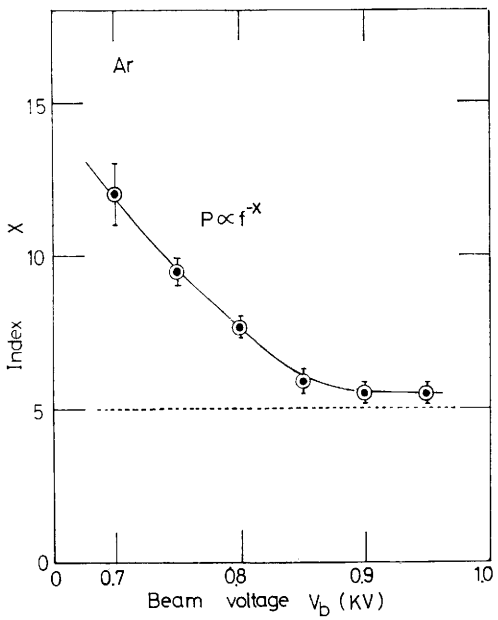

Fig. 12. Index x is plotted as a function of V_b. $I_d = 155$ mA.

In Fig. 11, the power P, thus obtained is plotted as a function of receiving frequency f with V_b as a parameter. It is noted that the power P can be expressed approximately by $P(f) \propto f^{-x}$, and the value of x decreases with increasing V_b. In Fig. 12, the variation of the value of x is shown as a function of V_b. It is seen there that it decreases and asymptotes to $x=5$, as V_b increases.

3.4 *Diffusion of the plasma across the magnetic field*

In order to obtain the feature of the density distribution along the radial direction, we observed the ion saturation current I_i by using the movable probe II (where the potential of probe is set at -75 V, while the space potential of plasma is about -25 V). An example of the results is shown in Fig. 13 (a), which shows that the plasma density decreases exponentially with r except the region of $r<5$ mm where the plasma is directly diffused from the discharge region along the magnetic field. We can obtain the e-folding length l of the plasma density from this figure. When the intensity of the beam is varied, l varies, and its behavior is shown in Fig. 13. (b), which shows that l is increased when V_b increases over a certain value. Since the more particles should diffuse across the magnetic field, for the larger l, the experimental result shown in Fig. 13 (b) means that when the intensity of the beam is

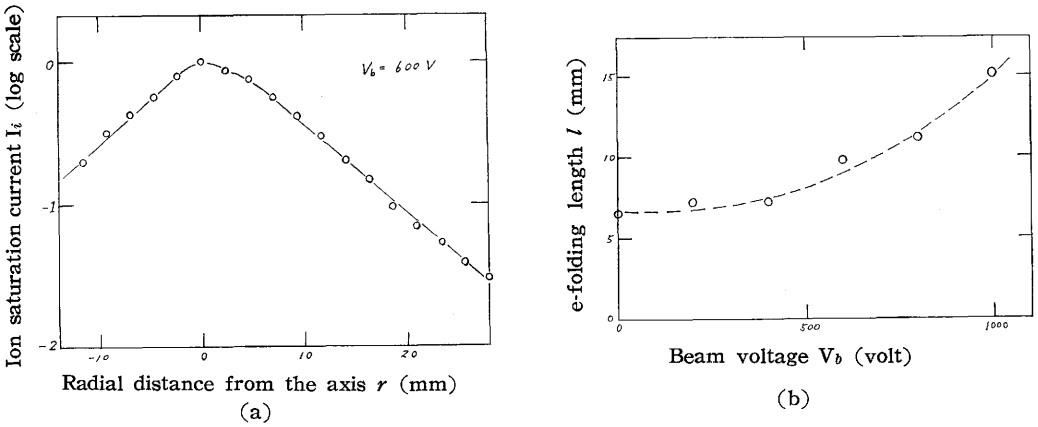

Fig. 13. (a) Typical feature of the density distribution $n(r)$ along the radial directrion and (b) e-foldinf length l of $n(r)$ as functions of V_b with B as a parameter. Ar, $p_2 = 7 \times 10^{-4}$ *Torr*. $I_d = 450$ *mA*. $f_c = 2.4$ *GHz*.

increased over a certain value of V_b, the diffusion of the plasma across the field increases rapidly.

4 Discussions

As described in Ref. 8, when the weak electron beam is injected into the plasma in nearly thermal equilibrium, the Bernstein mode is excited strongly and the behavior of it can be explained fairly well by the dispersion relation derived from the linear approximation. However, it is shown in § 3 of this paper that in the case of the more intense electron beam, the harmonics of this mode, as well as the fundamental mode, are excited as the results of the nonlinear interation among the waves grown to very large amplitude in the beam-plasma system. The feature of harmonic waves which is quite different from that of the fundamental wave is that they can not propagate into the plasma region across the boundary of the beam region and are confined in the beam-plasma region as shown in Fig. 5. This fact may be interpreted as follows : the fundamental wave (the Bernstein mode) is the characteristic wave of the plasma so that it can propagate in the plasma region, while the harmonic waves are not characteristic for the same plasma so that they can be generated in the beam-plasma system but can not propagate into the plasma region. Though the latter waves may propagate as far as a several wevelengths in the plasma region by the tunneling effect, the distance corresponding to them is very short because of the large propagation constant $k_\perp$, as shown in Ref. 8.

It is considered from Fig. 6, that along the z axis, the beam-plasma system is divided into two regions ; the 'linear' region where the fundamental wave grows exponentially, that is, $0 < z < z_{sa,1}$ and the 'nonlinear' region where the power for the fundamental wave reaches its saturation level and the harmonic waves are generated, that is, $z_{sa,1} < z$. As shown in Fig. 8, the growth rate k_i of the fundamental wave in the former region increases with increasing the intensity of the beam. This result is consistent with that of Levitsskii et al[10].

It is pressumed from Fig. 9, in which the peaks of fundamental and harmonic waves decay and are broadened in the nonlinear region, that the energy distribution function of the electron beam decays and parhaps reaches plateau stage by the nonlinear interaction as indicated by the quasilinear theory[11]. However, the energy distribution can not be measured for the structure of the apparatus where the energy analizer can not be inserted because the plasma and the beam sources are situated at the both side of it.

As shown in Figs. 10, 11 and 12, in the nonlinear region, the emission power P can be expressed approximately by $P(f) \propto f^{-x}$, and the value of x decreases and reaches about 5 as V_b increases. On the other hand, it has been shown theoretically[12], that the spectrum of the density fluctuation $P(k)$ must be proportional to k^{-5} in a turbulent low β plasma, where k is a wave number. In our case, if it is assumed that the harmonic waves have the same velocity, the above equation of power spectrum reduces to $P(k) \propto k^{-5}$. This assumption is considered to be reasonable, because the harmonics are generated by the electron beam and their phase velocity are equal to the velosity of the beam. Thus, if the Chen's remark is applicable to our case, it may be said from the above mentioned results that the beam-plasma system under study becomes turbulent when the intensity of the electron beam is increased.

On the other hand, it is known by comparing Fig. 13 (b) with Figs. 10 and 11, that the diffusion of the plasma is increased rapidly, when the intensity of the beam is increased over the nonlinear region. This fact may be considered to support the abive description that the turbulent state is attained when the beam intensity becomes intense.

Since the starting length z_{st} and the saturation length z_{sa} of the fundamental and the harmonic waves become small with increasing the intensity of the beam, as shown in Fig. 7, the measuring the emission power at the fixed point on the axis with increasing the intensity of the beam may be considered to be consistent with the measuring at the fixed intensity of the beam with increasing the axitial distance z. If we consider this saying, the experimental results where the beam intensity is varied may be considered to be those where the axitial distance z is varried at the fixed beam intensity.

After all, it is concluded that when the fairly intense electron beam is injected into the plasma in nearly thermal equilibrium, the Bernstein mode grows exponentially along the z axis, reaches its saturation level together with the generation of the harmonics confined in the beam-plasma region and then these waves decay and their spectra become broadened, the system removing to the turbulence-like state with the diffusion of the ion. A part of this conclusion are quite similar to Apel's experiment reported recently where the fundamental wave is not the Bernstein mode but the plasma wave derived by assuming cold plasma.

References

1) E. G. Harris : Phys. Rev. Letters **2** (1959) 34 ; J. nuclear Energy Part C **2** (1961) 138.
2) E. Canobbio and R. Croci : Proc. 6th Intern. Conf. on Phenomena in Ionized Gases, Paris (SERMA Publ. Co., Paris, 1964) Vol. 3, 269 ; Phys. of Fluids **9** (1966) 549.

3) F. W. Crawford and J. A. Tataronis : Proc. 7th Intern. Conf. on Phenomena in Ionized Gases, Beograde (Gradevinska Knjiga Publ. Hause, Beograde ; 1966) Vol. 2, p 715 and J. appl. Phys. **36** (1965) 2930.
4) G. Landauer : J. nuclear Energy Part C **4** (1962) 395.
5) K. Mitani, H. Kubo and S. Tanaka : J. Phys. Soc. Japan **19** (1964) 211, 221 and **20** (1965) 462.
6) S. Gruber, M. D. MacBee and L. T. Shepherd : Appl. Phys. Letters **4** (1964) 137.
7) G. Bekefi and E. B. Hooper : Appl. Phys. Letters **4** (1964) 135.
8) T. Idehara, K. Ohkubo and S. Tanaka : J. Phys. Soc. Japan **27** (1969) 187.
9) J. R. Apel : Phys. of Fluids **12** (1969) 291 and 640.
10) S. M. Levitskii and I. P. Shashurin : Soviet Physics JETP **25** (1967) 227.
11) V. D. Shapiro : Soviet Physics JETP **17** (1963) 416.
V. D. Shapiro and V. I. Shevchenko : Soviet Physics JETP **27** (1968) 635.
12) F. F. Chen : Phys. Rev. Letters **15** (1965) 381.